

Imageneseq+

panel para el diagnóstico molecular + comprehensivo

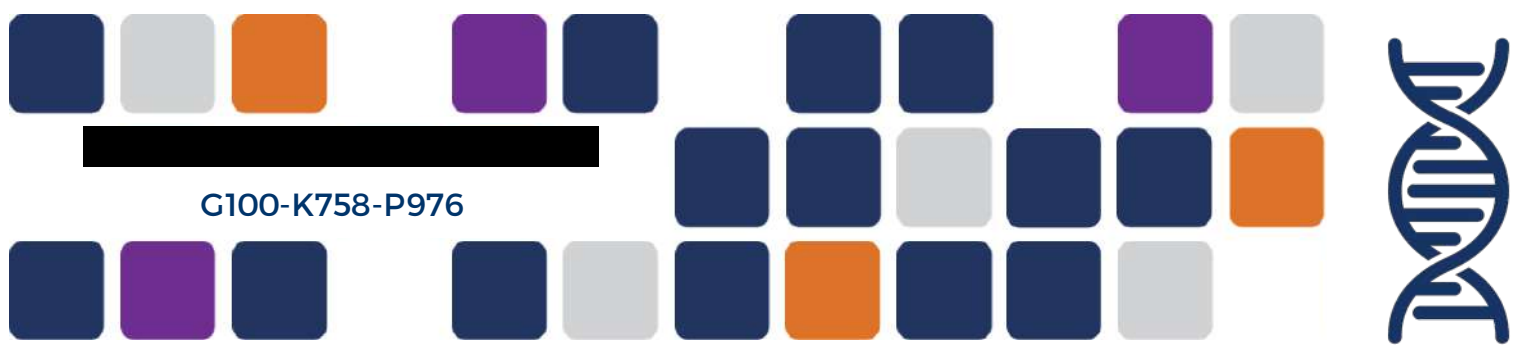
Reporte Clínico

Paciente:



Imageneseq Health ID:





G100-K758-P976

Patient

G100-K758-P976

Requestor

Doctors Hospital

Panel

ImageneSeq+

Glioblastoma Multiforme (IV)
03/16/2021

Hallazgos Clínicamente Relevantes

Variantes con Nivel de Evidencia 1

Symbol	Cancer Type	Targeted Drugs	Clinical Significance	Evidence Level
FGFR3-TACC	Carcinoma Urotelial	Erdafitinib	Terapéutico	1A

Variantes con Nivel de Evidencia 2

Symbol	Cancer Type	Targeted Drugs	Clinical Significance	Evidence Level
FGFR3-	Glioblastoma Multiforme	Erdafitinib	Sensible	2D
TACC	Carcinoma adrenal	Erdafitinib	Sensible	2D

Perfil molecular para inmunoterapia

TMB	MS	MMR
10 mutations/Mb	Stable 0.1379	Eficiente

Defined low TMB as ≤ 5 , intermediate TMB > 5 and < 20 , high TMB as ≥ 20 and < 50 , and very high TMB as ≥ 50 mutations/Mb

Resumen del Reporte ImageneSeq+

Los estudios clínicos disponibles en pacientes con GBM de genotipo similar, demuestran disminución de la progresión tumoral, aún después de haber fallado a tratamiento con temozolomide. Esta respuesta también se ha confirmado en otros tumores como carcinomas uroteliales con fusiones FGFR3-TACC, indicando la posibilidad de beneficio terapéutico con erdafitinib en el paciente. alelos normales de IDH1 y IDH2. Como las mutaciones en IDH1/2 se observan en gliomas de bajo grado, este resultado apoya a nivel molecular la observación de un alto grado de anaplasia celular que se observó histológicamente. En conjunto, el patrón genético descrito es concluyente con un diagnóstico molecular de glioblastoma multiforme tipo RTKII, según la clasificación WHO-2016. La mutación en PTEN confiere mal pronóstico en GBM-RTKII.



MUTACIONES TIPO III:

Variantes de significado clínico incierto

GENE	VARIATION	VARIATION TYPE	FREQUENCY	SIFT	POLYPHEN2	FUNCTIONAL IMPLICATION
FGFR3	c.-102-3T>C	splice_region_variant intron_variant	100.0%	NA	NA	Uncertain
MT-CYB	p.T71/c.20C>T	missense_variant	100.0%	NA	NA	Uncertain
WRN	c.1982-5delT	splice_region_variant intron_variant	98.72%	NA	NA	Benign
RECQL4	c.2295+1delC	splice_acceptor_variant splice_donor_variant intron_variant	96.82%	NA	NA	Uncertain
KMT2B	p.R1021fs/c.3059dupG	frameshift_variant splice_region_variant	94.6%	NA	NA	Uncertain
RECQL4	p.R766G/c.2296C>G	missense_variant splice_region_variant	79.78%	NA	NA	Uncertain
KMT2B	p.R855Q/c.2564G>A	missense_variant	57.74%	T	P	Uncertain
ABCC3	p.T809M/c.2426C>T	missense_variant	56.22%	D	D	Uncertain
GLI2	p.Q1176H/c.3528G>T	missense_variant	55.29%	NA	D	Benign
LRP1B	c.12805+4A>C	splice_region_variant intron_variant	52.7%	NA	NA	Uncertain
CDK9	c.617-7G>A	splice_region_variant intron_variant	50.49%	NA	NA	Uncertain
ASXL1	p.K838R/c.2513A>G	missense_variant	49.88%	T	P	Benign
CYP1A1	p.T394R/c.1181C>G	missense_variant	48.79%	D	D	Uncertain
NBN	p.D469Y/c.1405G>T	missense_variant	48.03%	D	D	Uncertain
DYNC2H1	p.G2577*/c.7729G>T	stop_gained	47.37%	T	NA	Uncertain
MSH3	p.A61_P63dup/c.181_189dupGCAGCC CCC	inframe_insertion	44.88%	NA	NA	Uncertain
SPTA1	p.A957V/c.2870C>T	missense_variant	41.57%	T	P	Benign
STAG2	c.1018-3delT	splice_region_variant intron_variant	40.0%	NA	NA	Uncertain
NOTCH4	p.L16dup/c.45_47dupG CT	disruptive_inframe_insertion	33.81%	NA	NA	Uncertain
AR	p.Q80dup/c.237_239dupGCA	disruptive_inframe_insertion	28.39%	NA	NA	Uncertain
SLIT2	p.R424W/c.1270C>T	missense_variant	27.36%	D	D	Uncertain
ZNF703	p.A513_A514dup/c.1537_1542dupGCC GCC	inframe_insertion	25.63%	NA	NA	Uncertain
CSMD1	p.W1094*/c.3281G>A	stop_gained	24.45%	T	NA	Uncertain
KDM5A	c.2151-4G>T	splice_region_variant intron_variant	20.1%	NA	NA	Uncertain
PRSS1	p.F73L/c.219T>A	missense_variant	17.2%	T	NA	Uncertain
FGFR1	p.N537H/c.1609A>C	missense_variant	16.88%	D	D	Uncertain
STAG2	c.2097-5delT	splice_region_variant intron_variant	15.7%	NA	NA	Uncertain



NPM1	c.847-5delT	splice_region_variant intron_variant	13.49%	NA	NA	Uncertain
ATM	c.1236-3dupT	splice_acceptor_variant intron_variant	10.73%	NA	NA	Benign
ATM	c.2922-8delT	splice_region_variant intron_variant	10.47%	NA	NA	Benign
MPL	p.I185R/c.554T>G	missense_variant	10.2%	D	P	Uncertain
PRSS3	p.G208G/c.624T>C	splice_region_variant synonymous_variant	9.79%	NA	NA	Uncertain
STAG2	c.2097-6_2097-5delTT	splice_region_variant intron_variant	9.09%	NA	NA	Uncertain
KDM6A	c.2724-5delT	splice_region_variant intron_variant	8.85%	NA	NA	Uncertain
CIC	p.K1375Q/c.4123A>C	missense_variant	8.55%	D	D	Uncertain
SOX9	p.K242Q/c.724A>C	missense_variant	8.17%	D	D	Uncertain
FOXP1	c.*56delA	splice_region_variant	8.16%	NA	NA	Uncertain
MSH2	c.212-4dupT	splice_region_variant intron_variant	7.87%	NA	NA	Benign
STAG2	c.2359-7delT	splice_region_variant intron_variant	7.83%	NA	NA	Uncertain
GPR124	c.2747+8C>G	splice_region_variant intron_variant	7.63%	NA	NA	Uncertain
FGFR4	p.R401P/c.1202G>C	missense_variant	7.47%	T	D	Uncertain
ATM	c.497-4delT	splice_region_variant intron_variant	7.27%	NA	NA	Benign
SPEN	c.1750-5dupT	splice_region_variant intron_variant	5.97%	NA	NA	Benign
MET	c.2638-9dupT	splice_region_variant intron_variant	5.9%	NA	NA	Uncertain
BRD4	p.E411A/c.1232A>C	missense_variant	5.73%	D	P	Uncertain
RHBDF2	p.C608W/c.1824T>G	missense_variant	5.66%	D	D	Uncertain
KMT2D	p.T4629P/c.13885A>C	missense_variant	5.56%	D	D	Uncertain
NF1	c.3198-4delT	splice_region_variant intron_variant	5.0%	NA	NA	Benign
ATM	c.1236-3delT	splice_region_variant intron_variant	4.88%	NA	NA	Benign
POLD1	c.1776-5delT	splice_region_variant intron_variant	4.8%	NA	NA	Uncertain
DYNC2H1	c.3574-8delT	splice_region_variant intron_variant	4.75%	NA	NA	Benign
RB1	c.1422-8delT	splice_region_variant intron_variant	4.68%	NA	NA	Benign
MSH6	c.3557-4dupT	splice_region_variant intron_variant	4.55%	NA	NA	Benign
RECQL4	c.2463+8delC	splice_region_variant intron_variant	4.45%	NA	NA	Uncertain
U2AF1	p.G219V/c.656G>T	missense_variant	4.45%	T	D	Uncertain
IRF2	c.88-3C>T	splice_region_variant intron_variant	4.44%	NA	NA	Uncertain
TSC1	c.2626-3C>T	splice_region_variant intron_variant	4.44%	NA	NA	Uncertain
CYP2D6	p.Y355C/c.1064A>G	missense_variant	4.38%	D	D	Uncertain
MSH6	c.3557-4delT	splice_region_variant intron_variant	4.2%	NA	NA	Benign
HDAC2	p.S75del/c.221_223delG CA	inframe_deletion	4.16%	NA	NA	Uncertain



MSH2	c.212-4delT	splice_region_variant intron_variant	4.12%	NA	NA	Benign
KMT2C	c.7443-5A>T	splice_region_variant intron_variant	4.04%	NA	NA	Uncertain
NPM1	c.139-9dupT	splice_region_variant intron_variant	4.0%	NA	NA	Uncertain
LRRK2	c.6844-8dupT	splice_region_variant intron_variant	3.98%	NA	NA	Uncertain
PMS2	c.706-3C>T	splice_region_variant intron_variant	3.94%	NA	NA	Uncertain
BRAF	c.2128-5dupT	splice_region_variant intron_variant	3.91%	NA	NA	Conflicting
ERBB2	c.1022-7T>A	splice_region_variant intron_variant	3.78%	NA	NA	Likely benign
IRF2	c.88-4delT	splice_region_variant intron_variant	3.66%	NA	NA	Uncertain
FLT3	c.1419-4dupT	splice_region_variant intron_variant	3.51%	NA	NA	Uncertain
PBRM1	c.996-4G>T	splice_region_variant intron_variant	3.42%	NA	NA	Uncertain
CNTNAP2	c.551-8delT	splice_region_variant intron_variant	3.42%	NA	NA	Uncertain
ABCC6	c.1636-2A>C	splice_acceptor_variant intron_variant	3.4%	NA	NA	Uncertain
CDC42	c.231+6T>C	splice_region_variant intron_variant	3.22%	NA	NA	Uncertain
SPEN	p.M2539L/c.7615A>C	missense_variant	3.13%	T	D	Uncertain
PRSS1	c.242+4A>G	splice_region_variant intron_variant	3.13%	NA	NA	Uncertain
MAP3K1	p.T949del/c.2845_2847delACA	inframe_deletion	3.06%	NA	NA	Benign
PIK3R2	c.1809-7A>C	splice_region_variant intron_variant	3.05%	NA	NA	Uncertain
FLT1	c.1437-6delT	splice_region_variant intron_variant	3.02%	NA	NA	Uncertain
C1orf147	p.Q61H/c.183A>C	missense_variant	3.0%	D	NA	Uncertain
IKBKE	c.1836-5T>G	splice_region_variant intron_variant	3.0%	D	NA	Uncertain
SPEN	c.1750-5delT	splice_region_variant intron_variant	2.99%	NA	NA	Uncertain
SOX10	p.T240P/c.718A>C	missense_variant	2.95%	D	D	Uncertain
GNAQ	c.736-4C>T	splice_region_variant intron_variant	2.86%	NA	NA	Uncertain
FLCN	p.H92P/c.275A>C	missense_variant	2.86%	T	D	Uncertain
ATM	c.2922-8dupT	splice_region_variant intron_variant	2.82%	NA	NA	Likely benign
MED12	p.Q2089del/c.6265_6267delCAG	inframe_deletion	2.8%	NA	NA	Uncertain
RUNX2	p.G66fs/c.195dupA	frameshift_variant	2.72%	NA	NA	Uncertain
BUB3	p.N265K/c.795C>A	missense_variant	2.66%	T	D	Uncertain
SLX4	p.L1714W/c.5141T>G	missense_variant	2.65%	T	D	Uncertain
MEF2B	p.L276V/c.826T>G	missense_variant	2.65%	T	P	Uncertain
FANCD2	c.378-5delT	splice_region_variant intron_variant	2.63%	NA	NA	Benign
CNTNAP1	c.3475-4T>A	splice_region_variant intron_variant	2.63%	NA	NA	Uncertain
ATR	p.I2065L/c.6193A>C	missense_variant	2.62%	T	P	Uncertain



SUFU	p.Y99D/c.295T>G	missense_variant	2.62%	D	D	Uncertain
ARID1A	p.Q1334del/c.3999_4001delGCA	disruptive_inframe_deletion	2.49%	NA	NA	Uncertain
ABL1	p.K628del/c.1883_1885delAGA	disruptive_inframe_deletion	2.4%	NA	NA	Uncertain
CHD2	c.3734dupA	splice_donor_variant intron_variant	2.39%	NA	NA	Uncertain
PRKDC	c.3729+1T>C	splice_acceptor_variant splice_donor_variant intron_variant	2.37%	NA	NA	Uncertain
ATR	p.1774fs/c.2320dupA	frameshift_variant	2.36%	NA	NA	Likely pathogenic
PTK2	p.I1042L/c.3124A>C	missense_variant	2.36%	D	D	Uncertain
CHD4	p.K306T/c.917A>C	missense_variant	2.34%	D	D	Uncertain
SOX9	p.D244H/c.730G>C	missense_variant	2.34%	D	D	Uncertain
NOTCH3	p.N247H/c.739A>C	missense_variant	2.31%	D	D	Uncertain
BRD4	p.S42R/c.124A>C	missense_variant	2.3%	T	D	Uncertain
SOX9	p.P238fs/c.710dupC	frameshift_variant	2.29%	NA	NA	Uncertain
MMP9	p.T470P/c.1408A>C	missense_variant	2.24%	D	D	Uncertain
JAK2	c.1777-7dupT	splice_region_variant intron_variant	2.22%	NA	NA	Uncertain
TUBD1	c.1260-7C>T	splice_region_variant intron_variant	2.21%	NA	NA	Uncertain
SMARCA4	p.F806V/c.2416T>G	missense_variant	2.21%	D	P	Uncertain
PMS2	c.706-3delC	splice_region_variant intron_variant	2.16%	NA	NA	Uncertain
WRN	c.840-3delT	splice_region_variant intron_variant	2.15%	NA	NA	Uncertain
BUB3	c.266-9dupT	splice_region_variant intron_variant	2.14%	NA	NA	Uncertain
AKT1	c.567+8C>G	splice_region_variant intron_variant	2.1%	NA	NA	Uncertain
ABCB1	p.Y1087D/c.3259T>G	missense_variant	2.09%	D	D	Uncertain
JAK2	c.1777-7delT	splice_region_variant intron_variant	2.07%	NA	NA	Uncertain
CHEK1	p.T242fs/c.724dupA	frameshift_variant	2.06%	NA	NA	Uncertain
PRRT2	p.R217fs/c.649delC	frameshift_variant	2.06%	NA	NA	Uncertain
KDM5A	c.871-6dupT	splice_region_variant intron_variant	2.04%	NA	NA	Uncertain
POLD1	c.1384-3T>A	splice_region_variant intron_variant	2.03%	NA	NA	Uncertain



Lista completa de genes analizados

ABCB1	BCL2L2	CD79A	CUL3	ERBB2	FGFR2	HDAC1	KMT2A	MYCN	PIK3CB	REL	SOCS1	TWIST1	TGFBR1
ABCC1	BCL6	CD79B	CXCL10	ERBB3	FGFR3	HDAC2	KMT2B	MYD88	PIK3CG	RET	SOD2	TYMS	TP53
ABCC2	BCOR	CDA	CXCL8	ERBB4	FGFR4	HDAC3	KMT2C	MYO1B	PIK3R1	RHBDF2	SOX10	U2AF1	TUBD1
ABCC3	BCORL1	CDC25C	CXCR4	ERCC1	FH	HDAC4	KMT2D	NAT1	PIK3R2	RHEB	SOX17	UGT1A1	
ABCC4	BCR	CDC42	CYLD	ERCC2	FLCN	HDAC6	KRAS	NAT2	PLCG2	RICTOR	SOX2	UGT1A9	
ABCC6	BIRC5	CDC73	CYP19A1	ERCC3	FLT1	HDAC8	LMO1	NBN	PLK1	RNF43	SOX9	UMPS	
ABCG2	BLCAP	CDH1	CYP1A1	ERCC4	FLT3	HGF	LRP1B	NCOR1	PMS1	ROCK1	SPEN	VEGFA	
ABL1	BLK	CDK1	CYP1A2	ERCC5	FLT4	HIF1A	LRRK2	NF1	PMS2	ROS1	SPINK1	VEGFB	
ABL2	BLM	CDK12	CYP1B1	ERG	FOLR3	HNF1A	LYN	NF2	POLD1	RPS6KA1	SPOP	VHL	
ACTG1	BMPR1A	CDK2	CYP2A6	ERRF1	FOXA1	HOXB13	LZTR1	NFKBIA	POLE	RPS6KB1	SPTA1	WEE1	
ACVR1B	BRAF	CDK4	CYP2B6	ESR1	FOXA2	HRAS	MAGI2	NKX2-1	PPARG	RPTOR	SRC	WISP3	
ACVR2A	BRCA1	CDK5	CYP2C19	ETV1	FOXL2	HSD3B1	MAP2K1	NOTCH1	PPP2R5B	RRM1	STAG2	WNT1	
AIP	BRCA2	CDK6	CYP2C8	ETV4	FOXO1	HSP90AA1	MAP2K2	NOTCH2	PRDM1	RUNX1	STAT3	WNT5A	
AKT1	BRD3	CDK7	CYP2C9	ETV5	FOXP1	IDH1	MAP2K4	NOTCH3	PREX2	RUNX1T1	STAT4	WNT6	
AKT2	BRD4	CDK8	CYP2D6	ETV6	FRS2	IDH2	MAP3K1	NOTCH4	PRF1	RUNX2	STK11	WRN	
AKT3	BRIP1	CDK9	CYP2E1	EWSR1	FUBP1	IGF1	MAP4K1	NRAS	PRKAR1A	SATB2	STK4	WT1	
ALK	BTG1	CDKN1A	CYP3A4	EXT1	FYN	IGF1R	MAPK1	NRG1	PRKCE	SBDS	SUFU	XIAP	
AMER1	BTK	CDKN1B	CYP3A5	EXT2	GABRA6	IGF2	MAPK14	NSD1	PRKCG	SDHA	SYK	XPA	
APC	BUB1	CDKN1C	CYP4B1	EZH2	GATA1	IGF2R	MAPK8	NTRK1	PRKCI	SDHAF2	TAF1	XPC	
AR	BUB1B	CDKN2A	DAXX	FAM46C	GATA2	IKBKB	MAPK9	NTRK2	PRKDC	SDHB	TBX3	XPO1	
ARAF	BUB3	CDKN2B	DDB2	FANCA	GATA3	IKBKE	MAX	NTRK3	PRRT2	SDHC	TCF7L2	XRCC1	
ARAF	C11ORF30	CDKN2C	DDR2	FANCB	GATA4	IKZF1	MCL1	NUP93	PRSS1	SETD2	TEK	YES1	
ARFRP1	C17ORF108	CEBPA	DHFR	FANCC	GATA6	IL7R	MDM4	OPRM1	PRSS8	SF3B1	TERT	ZBTB2	
ARID1A	C8ORF34	CEP57	DICER1	FANCD2	GGH	INHBA	MED12	PAK1	PTCH1	SHH	TET2	ZNF217	
ARID1B	CAMK2G	CHD2	DIRAS3	FANCE	GID4	INPP4B	MEN1	PAK3	PTCH2	SLC10A2	TGFBR2	ZNF703	
ARID2	CAMKK2	CHD3	DIS3L2	FANCF	GLI1	IRF4	MET	PALB2	PTEN	SLC19A1	TLR4	BAX	
ASXL1	CARD11	CHD4	DNMT3A	FANCG	GLI2	IRS2	MITF	PARK2	PTK2	SLC22A16	TMEM127	CASP7	
ATIC	CASP8	CHEK1	DOT1L	FANCI	GNA11	ITK	MLH1	PARP1	PTPN11	SLC28A3	TMPRSS2	CHEK2	
ATM	CBFB	CIC	DPYD	FANCL	GNA13	JAK1	MMP12	PARP2	QKI	SLCO1B3	TNF	COPS3	
ATR	CBL	CNTNAP1	DYNC2H1	FANCM	GNAQ	JAK2	MMP14	PARP3	RAC1	SLIT2	TNFAIP3	CRLF2	
ATRX	CBR1	CNTNAP2	E2F1	FAS	GNAS	JAK3	MMP9	PARP4	RAC2	SLX4	TNFRSF11A	IRF2	
AURKA	CBR3	COL22A1	EGF	FAT1	GOPC	JUN	MPL	PAX5	RAD50	SMAD2	TNFRSF14	MDM2	
AURKB	CCND1	COMT	EGFR	FBXW7	GPC3	KAT6A	MRE11A	PBRM1	RAD51D	SMAD3	TNFSF11	MEF2B	
AXIN1	CCND2	CREBBP	EML4	FCGR3A	GPR124	KDM5A	MSH2	PDCD1	RAF1	SMAD4	TOP1	MYB	
AXIN2	CCND3	CRKL	ENOSF1	FGF10	GRB2	KDM5C	MSH3	PDCD1LG2	RANBP2	SMARCA1	TOP2A	NFE2L2	
AXL	CCNE1	CSF1R	EP300	FGF14	GRIN2A	KDM6A	MSH6	PDGFRA	RARA	SMARCA4	TPMT	NPM1	
BAP1	CD19	CSMD1	EPCAM	FGF19	GRM3	KDR	MTHFR	PDGFRB	RARB	SMARCB1	TSC1	PPP2R1A	
BARD1	CD22	CSMD3	EPHA3	FGF23	GSK3B	KEAP1	MTOR	PDK1	RASSF1	SMARCD1	TSC2	RAD51	
BCL10	CD274	CTCF	EPHA5	FGF3	GSTA1	KEL	MTR	PEG3	RASSF8	SMO	TSHR	RAD51C	
BCL11A	CD33	CTLA4	EPHA7	FGF4	GSTM3	KIAA0427	MUTYH	PHOX2B	RB1	SNAI1	TUBA1A	RHOA	
BCL2	CD52	CTNNA1	EPHB1	FGF6	GSTP1	KIT	MYC	PIK3C2B	RBM10	SNAI2	TUBB	SDHD	
BCL2L1	CD74	CTNNB1	EPHX1	FGFR1	H3F3A	KLHL6	MYCL	PIK3CA	RECQL4	SNCAIP	TUBE1	SLC16A7	



Control de calidad

Quality control of the sequencing project

Imagen Health ID	LibID	Raw bases(G)	Raw Reads	Q30(%)
██████████	FIPM190008364-1A	11.43	76.98 M	93.06

Sequencing reads quality control

Library Peak Size(bp):	99.98	ReadNum_on_target_before_rmdup:	52931052
Library 25%~75% Size(bp):	1791.54	ReadNum_on_target_after_rmdup:	38680651
Coverage_of_target_region(%):	42.73	BaseNum_on_target_after_rmdup(Mb):	4818.82
Average_sequencing_depth_on_target:	24.77	BaseNum_covered_on_target(bp):	2689202
Data_effective_ratio(%):	26.92	Fraction_of_target_covered_with_at_least_10x(%):	99.92
Duplication_rate_whole_genome(%):	59.29	Fraction_of_target_covered_with_at_least_30x(%):	99.76
Duplication_rate_on_target(%):	57.45	Fraction_of_target_covered_with_at_least_50x(%):	99.59
Probe_capture_ratio_Before_Rmdup(%):	11277.39	Fraction_of_target_covered_with_at_least_100x(%):	99.12
Probe_capture_ratio_After_Rmdup(%):	75793830	Fraction_of_target_covered_with_at_least_200x(%):	97.94
Total_Bases_num_in_bam(Mb):	75594453	Fraction_of_target_covered_with_at_least_500x(%):	92.66
Total_reads_num_in_bam:	99.74	Fraction_of_target_covered_with_at_least_1000x(%):	78.44
Mapped_reads_num:	0.2925	Fraction_of_target_covered_with_at_least_1500x(%):	58.94
Mapping_rate(%):	0.4575	Fraction_of_target_covered_with_at_least_2000x(%):	38.01
Mismatch_rate_in_target_region(%):	2689765	Zero_PeakDepth_Flag:	0
Mismatch_rate_in_all_effective_sequence(%):	56819626	Average_TargetDepth:	1791.54
Target_region_size(bp):	8388.54	Peak_Depth:	1716
Total_reads_num_after_rmdup:	148.79	Peak_Depth_Shift(%):	4.22
Total_mapped_baseNum_after_rmdup(Mb):	99.98	Standard_Deviation_of_Depth:	968.13
Average_read_length(bp):	1791.54	Normalized_Standard_Deviation_of_Depth:	54.04



REFERENCIAS

1. Reifenger G, Wirsching HG, Knobbe-Thomsen CB, Weller M: Advances in the molecular genetics of gliomas - implications for classification and therapy. *Nat Rev Clin Oncol* 2017;14:434-452
2. Masui K, Mischel PS, Reifenger G: Molecular classification of gliomas. *Handb Clin Neurol* 2016;134:97-120
3. Louis DN, Perry A, Reifenger G, von Deimling A, Figarella-Branger D, Cavenee WK, Ohgaki H, Wiestler OD, Kleihues P, Ellison DW: The 2016 World Health Organization Classification of Tumors of the Central Nervous System: a summary. *Acta Neuropathol* 2016;131:803-820
4. Singh D, Chan JM, Zoppoli P, Niola F, Sullivan R, Castano A, Liu EM, Reichel J, Porrati P, Pellegatta S, Qiu K, Gao Z, Ceccarelli M, Riccardi R, Brat DJ, Guha A, Aldape K, Golfinos JG, Zagzag D, Mikkelsen T, Finocchiaro G, Lasorella A, Rabadan R, Iavarone A: Transforming fusions of FGFR and TACC genes in human glioblastoma. *Science (New York, NY)* 2012;337:1231-1235
5. Lasorella A, Sanson M, Iavarone A: FGFR-TACC gene fusions in human glioma. *Neuro Oncol* 2017;19:475-483
6. Di Stefano AL, Fucci A, Frattini V, Labussiere M, Mokhtari K, Zoppoli P, Marie Y, Bruno A, Boisselier B, Giry M, Savatovsky J, Touat M, Belaid H, Kamoun A, Idbaih A, Houillier C, Luo FR, Soria J-C, Tabertero J, Eoli M, Paterra R, Yip S, Petrecca K, Chan JA, Finocchiaro G, Lasorella A, Sanson M, Iavarone A: Detection, Characterization, and Inhibition of FGFR-TACC Fusions in IDH Wild-type Glioma. *Clinical cancer research: an official journal of the American Association for Cancer Research* 2015;21:3307-3317
7. Libermann TA, Nusbaum HR, Razon N, Kris R, Lax I, Soreq H, Whittle N, Waterfield MD, Ullrich A, Schlessinger J: Amplification, enhanced expression and possible rearrangement of EGF receptor gene in primary human brain tumours of glial origin. *Nature* 1985;313:144-147
8. Westphal M, Maire CL, Lamszus K: EGFR as a Target for Glioblastoma Treatment: An Unfulfilled Promise. *CNS Drugs* 2017;31:723-735
9. An Z, Aksoy O, Zheng T, Fan QW, Weiss WA: Epidermal growth factor receptor and EGFRvIII in glioblastoma: signaling pathways and targeted therapies. *Oncogene* 2018;37:1561-1575
10. Thorne AH, Zanca C, Furnari F: Epidermal growth factor receptor targeting and challenges in glioblastoma. *Neuro Oncol* 2016;18:914-918
11. Chinot OL, Wick W, Mason W, Henriksson R, Saran F, Nishikawa R, Carpentier AF, Hoang-Xuan K, Kavan P, Cernea D, Brandes AA, Hilton M, Abrey L, Cloughesy T: Bevacizumab plus radiotherapy-temozolomide for newly diagnosed glioblastoma. *The New England journal of medicine* 2014;370:709-722
12. Cloughesy TF, Yoshimoto K, Nghiemphu P, Brown K, Dang J, Zhu S, Hsueh T, Chen Y, Wang W, Youngkin D, Liao L, Martin N, Becker D, Bergsneider M, Lai A, Green R, Oglesby T, Koletto M, Trent J, Horvath S, Mischel PS, Mellinghoff IK, Sawyers CL: Antitumor activity of rapamycin in a Phase I trial for patients with recurrent PTEN-deficient glioblastoma. *PLoS Med* 2008;5:e8
13. Galanis E, Buckner JC, Maurer MJ, Kreisberg JI, Ballman K, Boni J, Peralba JM, Jenkins RB, Dakhil SR, Morton RF, Jaeckle KA, Scheithauer BW, Dancey J, Hidalgo M, Walsh DJ: Phase II trial of temsirolimus (CCI-779) in recurrent glioblastoma multiforme: a North Central Cancer Treatment Group Study. *Journal of clinical oncology : official journal of the American Society of Clinical Oncology* 2005;23:5294-5304
14. Hainsworth JD, Shih KC, Shepard GC, Tillinghast GW, Brinker BT, Spigel DR: Phase II study of concurrent radiation therapy, temozolomide, and bevacizumab followed by bevacizumab/everolimus as first-line treatment for patients with glioblastoma. *Clin Adv Hematol Oncol* 2012;10:240-246



Imagene Health

Contact Info

+52(811)611-6514

imagenehealth.com

info@imagenehealth.com

Ave. Vasconcelos 430, Plaza Tribeca L134, San Pedro, NL 66220

